

Quantitative evaluations of stability and convergence for solutions of semilinear Klein–Gordon equation

Takuya Tsuchiya^{*1} and Makoto Nakamura²

¹Faculty of Economics, Meiji Gakuin University, Japan

²Department of Pure and Applied Mathematics, Graduate School of Information Science and Technology, The University of Osaka, Japan

March 10, 2026

Abstract

We perform some simulations of the semilinear Klein–Gordon equation with a power-law nonlinear term and propose each of the quantitative evaluation methods for the stability and convergence of numerical solutions. We also investigate each of the thresholds in the methods by varying the amplitude of the initial value and the mass, and propose appropriate values.

1 Introduction

Many natural phenomena are expressed by (nonlinear) hyperbolic equations. We are strongly interested in the behavior of the asymptotic solutions of the equations in time. In addition, the properties of the solutions should be changed in a curved spacetime since the differential operator is affected by the curvature of spacetime (e.g.[1]). We adopt the Klein–Gordon equation as the hyperbolic equation since it can be applied to a curved spacetime. Some analytical results of the equation in the de Sitter spacetime, which is one of the curved spacetimes, have been reported [2, 3]. Regarding the numerical study of the equation, we have reported the numerical solutions of the equation in the de Sitter spacetime using the structure-preserving scheme [4], suggested some discrete equations constructed using the structure-preserving scheme [5], and investigated the reasons for the difference in stability between the discrete equations [6].

In (partial) differential equations, the stability and convergence of numerical solutions are necessary for the correctness of the solutions. Although we have proposed highly accurate numerical solutions for the semilinear Klein–Gordon equation [4, 5, 6], we have not quantitatively evaluated the stability and convergence of the solutions. In this paper, we propose some quantitative evaluation methods for the stability and convergence of the solutions for the semilinear Klein–Gordon equation in the flat spacetime.

Indices such as (i, j, \dots) run from 1 to n , where n is the spatial dimension. We use the Einstein convention of summation of repeated up–down indices in this paper.

2 Semilinear Klein–Gordon equation

The semilinear Klein–Gordon equation with the power-law nonlinear term in the flat spacetime is

$$-\frac{1}{c^2} \partial_t^2 \phi + \delta^{ij} (\partial_i \partial_j \phi) - \frac{c^2 m^2}{\hbar^2} \phi = \lambda |\phi|^{p-1} \phi, \quad (1)$$

where ϕ is the dynamical variable, δ^{ij} is the Kronecker delta, m is the mass, c is the speed of light, \hbar is the Dirac constant, p is an integer larger than 2, and λ is a constant and has a physical dimension of $1/(\text{length})^2$. When performing numerical calculations, the canonical form is preferable since it is a system of first-order equations in

^{*}tatsuchi@eco.meijigakuin.ac.jp

time. Moreover, it is easy to confirm the accuracy of the numerical calculations since there is a constraint with respect to time such as the total Hamiltonian. The Hamiltonian density of (1) is given by

$$\mathcal{H} = \frac{L_0}{2} \left(\frac{\psi^2}{L_0^2} + \delta^{ij} (\partial_i \phi) (\partial_j \phi) + \frac{c^2 m^2 \phi^2}{\hbar^2} + \frac{2\lambda |\phi|^{p+1}}{p+1} \right), \quad (2)$$

where L_0 is a constant value that makes the physical dimension of \mathcal{H} into an energy dimension and ψ is the canonical momentum of ϕ . Then, the canonical equations of (1) are

$$\frac{1}{c} \partial_t \phi = \frac{1}{L_0} \psi, \quad (3)$$

$$\frac{1}{c} \partial_t \psi = L_0 \delta^{ij} (\partial_i \partial_j \phi) - \frac{L_0 c^2 m^2}{\hbar^2} \phi - L_0 \lambda |\phi|^{p-1} \phi. \quad (4)$$

The discretized equations of (2), (3), and (4) can be respectively defined as

$$\mathcal{H}_{(\mathbf{k})}^{(\ell)} := \frac{L_0}{2} \left(\frac{(\psi_{(\mathbf{k})}^{(\ell)})^2}{L_0^2} + \delta^{ij} (\widehat{\delta}_i^{(1)} \phi_{(\mathbf{k})}^{(\ell)}) (\widehat{\delta}_j^{(1)} \phi_{(\mathbf{k})}^{(\ell)}) + \frac{c^2 m^2}{\hbar^2} (\phi_{(\mathbf{k})}^{(\ell)})^2 + \frac{2\lambda}{p+1} |\phi_{(\mathbf{k})}^{(\ell)}|^{p+1} \right), \quad (5)$$

$$\frac{\phi_{(\mathbf{k})}^{(\ell+1)} - \phi_{(\mathbf{k})}^{(\ell)}}{c\Delta t} := \frac{1}{2L_0} (\psi_{(\mathbf{k})}^{(\ell+1)} + \psi_{(\mathbf{k})}^{(\ell)}), \quad (6)$$

$$\frac{\psi_{(\mathbf{k})}^{(\ell+1)} - \psi_{(\mathbf{k})}^{(\ell)}}{c\Delta t} := L_0 \left(-\frac{\lambda}{p+1} \frac{|\phi_{(\mathbf{k})}^{(\ell+1)}|^{p+1} - |\phi_{(\mathbf{k})}^{(\ell)}|^{p+1}}{\phi_{(\mathbf{k})}^{(\ell+1)} - \phi_{(\mathbf{k})}^{(\ell)}} + \frac{\delta^{ij} \widehat{\delta}_i^{(1)} \widehat{\delta}_j^{(1)} (\phi_{(\mathbf{k})}^{(\ell+1)} + \phi_{(\mathbf{k})}^{(\ell)})}{2} - \frac{c^2 m^2 (\phi_{(\mathbf{k})}^{(\ell+1)} + \phi_{(\mathbf{k})}^{(\ell)})}{2\hbar^2} \right), \quad (7)$$

where (ℓ) means the time index, (\mathbf{k}) means the space index, and $\mathbf{k} = (k_1, \dots, k_n)$. $\widehat{\delta}_i^{(1)}$ is the first-order central difference operator defined as

$$\widehat{\delta}_i^{(1)} u_{(\mathbf{k})}^{(\ell)} := \frac{u_{(k_1, \dots, k_i+1, \dots, k_n)}^{(\ell)} - u_{(k_1, \dots, k_i-1, \dots, k_n)}^{(\ell)}}{2\Delta x^i}.$$

Note that (5)–(7) are called Form I in [6]. Here, Δx^i is the i th grid range. If $n = 3$, for example, $\Delta x^1 = \Delta x$, $\Delta x^2 = \Delta y$, and $\Delta x^3 = \Delta z$. The nonlinear term can be expressed as

$$\frac{|\phi_{(\mathbf{k})}^{(\ell+1)}|^{p+1} - |\phi_{(\mathbf{k})}^{(\ell)}|^{p+1}}{\phi_{(\mathbf{k})}^{(\ell+1)} - \phi_{(\mathbf{k})}^{(\ell)}} = \{ |\phi_{(\mathbf{k})}^{(\ell+1)}|^p + |\phi_{(\mathbf{k})}^{(\ell+1)}|^{p-1} |\phi_{(\mathbf{k})}^{(\ell)}| + \dots + |\phi_{(\mathbf{k})}^{(\ell+1)}| |\phi_{(\mathbf{k})}^{(\ell)}|^{p-1} + |\phi_{(\mathbf{k})}^{(\ell)}|^p \} \frac{|\phi_{(\mathbf{k})}^{(\ell+1)}| - |\phi_{(\mathbf{k})}^{(\ell)}|}{\phi_{(\mathbf{k})}^{(\ell+1)} - \phi_{(\mathbf{k})}^{(\ell)}}. \quad (8)$$

The total Hamiltonian $\int_{\mathbb{R}^n} \mathcal{H} dx^n$ at a discrete level is preserved using (6) and (7) [6].

3 Quantitative evaluations of stability and convergence

In this paper, the word “stable simulation” means that no vibration occurs in the waveform of ϕ . Moreover, to quantitatively evaluate stability, we define

$$d\phi_{(\mathbf{k})}^{(\ell)} := \widehat{s}_i^+ \phi_{(\mathbf{k})}^{(\ell)} - \phi_{(\mathbf{k})}^{(\ell)} \quad (9)$$

and sum of $|d\phi_{(\mathbf{k})}^{(\ell)}|/(\text{grid})$ if $d\phi_{(\mathbf{k})}^{(\ell)}$ satisfies the condition

$$(\widehat{s}_i^+ d\phi_{(\mathbf{k})}^{(\ell)}) d\phi_{(\mathbf{k})}^{(\ell)} < 0 \quad (10)$$

over \mathbf{k} , where \widehat{s}_i^+ is the discrete operator that shifts the space forward. We call this value SV_g , which is determined for each grid, and consider the simulation stable when SV_g is less than or equal to the threshold ε_s . SV_g represents the number of vibrations per grid weighted by $|d\phi_{(\mathbf{k})}^{(\ell)}|$. We study the appropriate value of ε_s in Section 4.

The word ‘‘convergence’’ means that ϕ approaches the exact solution with an increasing number of grids. To quantitatively determine convergence, we define the relative errors of ϕ :

$$CV_g(t) := \log_{10} \frac{\|\phi_g(x) - \phi_G(x)\|_2}{\|\phi_G(x)\|_2}, \quad (11)$$

where $\phi_g(x)$ is the value of ϕ for each grid number and $\phi_G(x)$ is that for the maximum grid number. Since (6) and (7) have the second-order convergence with respect to the number of grids [6], we define the difference in $CV_g(t)$ from the second-order convergence as

$$DCV_g(t) := \left| CV_{\bar{G}}(t) - CV_g(t) + \left(\log_2 \frac{\bar{G}}{g} \right) (\log_{10} 4) \right|, \quad (12)$$

where \bar{G} is the second largest grid number. If $DCV_g(t)$ is less than or equal to the threshold ε_c , we decide that the convergence of the simulation is satisfied. We also study the appropriate value of ε_c in Section 4.

4 Numerical results

In this section, we perform some simulations using the settings given below. The initial conditions are set as $\phi(x, \bar{x}) = \phi(x) = A \cos(2\pi x)$ and $\psi(x, \bar{x}) = \psi(x) = 2\pi A \sin(2\pi x)$ for $x \in \mathbb{R}$ and $\bar{x} \in \mathbb{R}^{n-1}$ with $A = 2, 3$ and $-1/2 \leq x \leq 1/2$. The boundary is periodic. The physical parameters are $c = \hbar = L_0 = 1$. The spatial dimension is $n = 3$. The grid ranges are $(\Delta x, \Delta t) = (1/250, 1/2500), (1/500, 1/5000), (1/1000, 1/10000), (1/2000, 1/20000), (1/4000, 1/40000),$ and $(1/8000, 1/80000)$. The simulation time is $0 \leq t \leq 1000$. The number of exponents of the nonlinear term is $p = 5$ and the coefficient parameter is $\lambda = 1$. The mass m ranges from 3.9 to 4.2 when $A = 2$ and from 7.6 to 8.2 when $A = 3$.

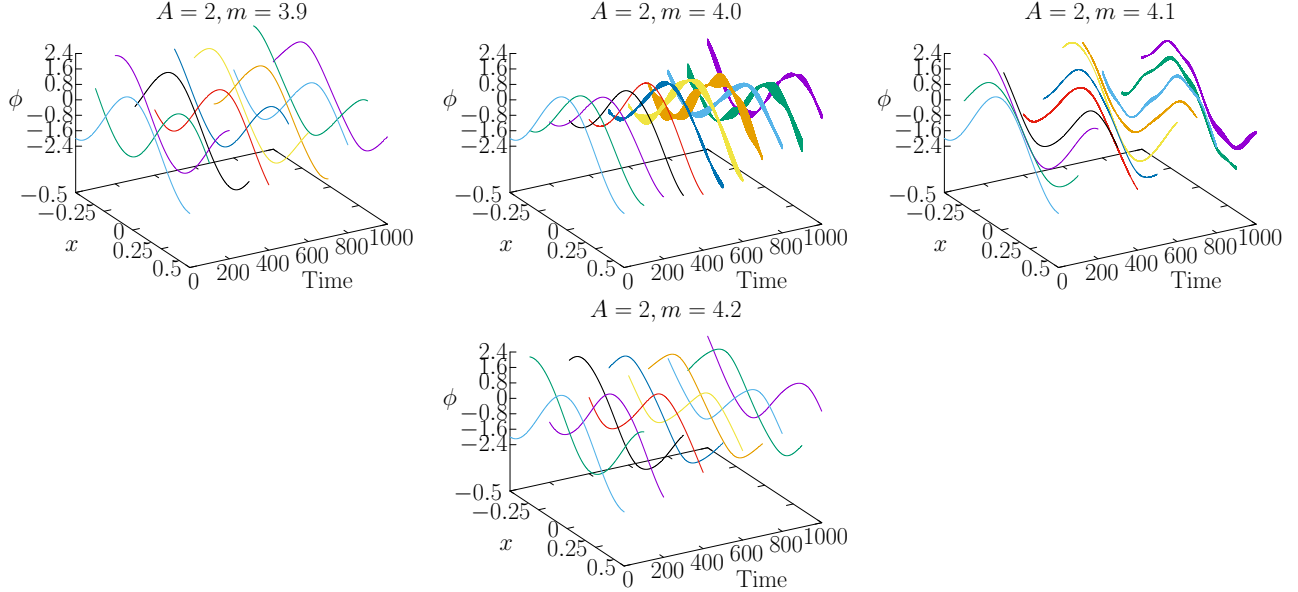


Figure 1: ϕ with $A = 2$, $m = 3.9$ to 4.2, and 8000 grids. The top-left panel is for $m = 3.9$, the top-center one is for $m = 4.0$, the top-right one is for $m = 4.1$, and the bottom one is for $m = 4.2$. The vibration appears to occur at $t \geq 500$ for $m = 4.0$ and at $t \geq 700$ for $m = 4.1$.

Fig. 1 shows ϕ with $A = 2$ and $m = 3.9$ to 4.2. The vibration seems to occur at $t \geq 500$ for $m = 4.0$ and at $t \geq 700$ for $m = 4.1$. On the other hand, no vibration appears to occur for $m = 3.9$ and 4.2. Fig. 2 shows ϕ with $A = 3$ and $m = 7.6$ to 8.2. The vibration seems to occur at $t \geq 900$ for $m = 7.8$, at $t \geq 300$ for $m = 7.9$, and at $t \geq 400$ for $m = 8.0$. On the other hand, no vibrations appear to occur for $m = 7.6, 7.7, 8.1,$ and 8.2.

To quantitatively evaluate stability, we investigate the appropriate value of ε_s . The value of ε_s is varied to 0.001, 0.06, 0.12, 0.18, 0.24, and 0.30. We summarize the results of the stability in Table 1. \bigcirc means that $SV_{8000} \leq \varepsilon_s$ is always satisfied at $0 \leq t \leq 1000$. On the other hand, the values represent the times when $SV_{8000} > \varepsilon_s$.

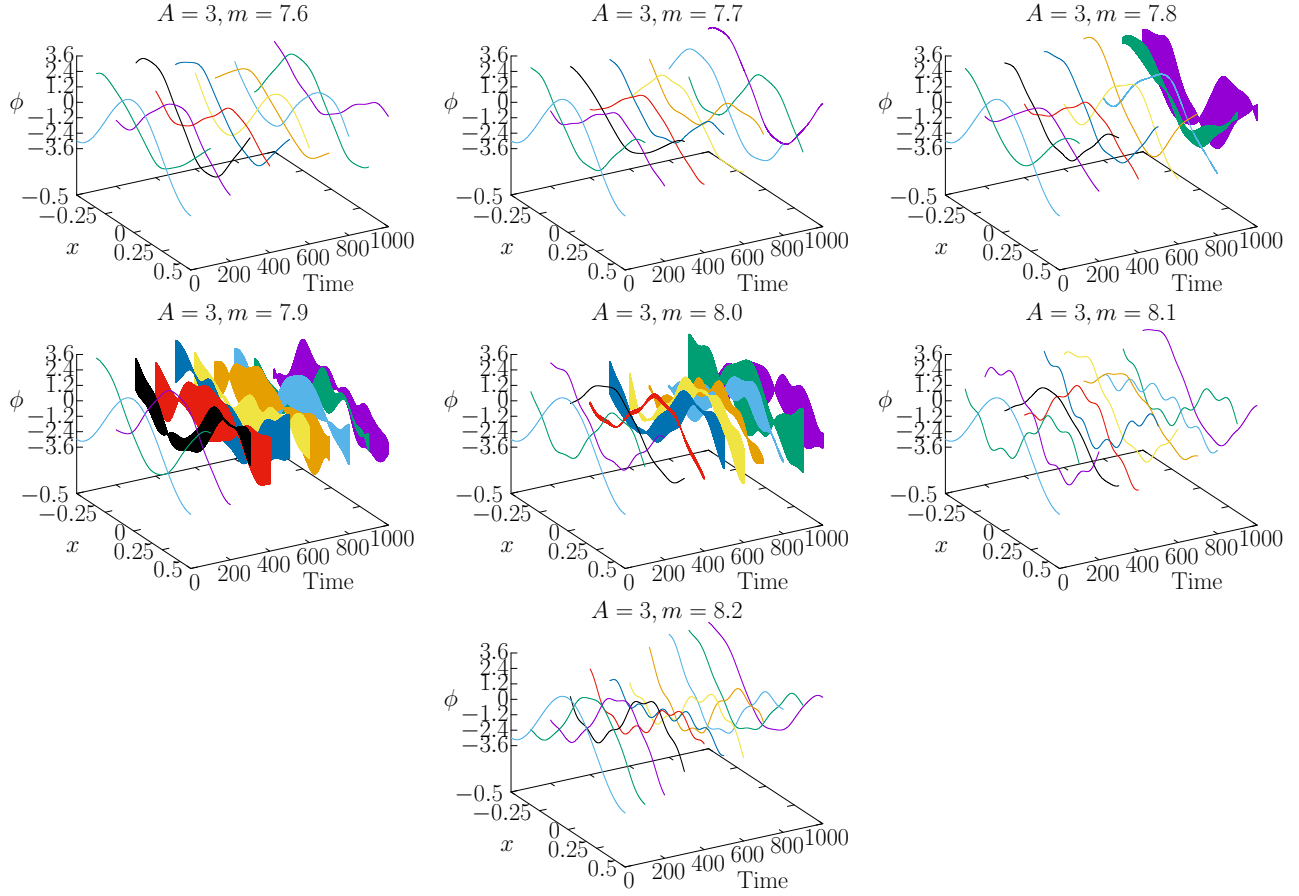


Figure 2: ϕ with $A = 3$, $m = 7.6$ to 8.2 , and 8000 grids. The top-left panel is for $m = 7.6$, the top-center one is for $m = 7.7$, the top-right one is for $m = 7.8$, the center-left one is for $m = 7.9$, the center one is for $m = 8.0$, the center-right one is for $m = 8.1$, and the bottom one is for $m = 8.2$. The vibration appears to occur at $t \geq 900$ for $m = 7.8$, at $t \geq 300$ for $m = 7.9$, and at $t \geq 400$ for $m = 8.0$.

$A = 2$					$A = 3$							
$\varepsilon_s \backslash m$	3.9	4.0	4.1	4.2	$\varepsilon_s \backslash m$	7.6	7.7	7.8	7.9	8.0	8.1	8.2
0.001	○	417	368	○	0.001	○	930	725	242	343	○	○
0.06	○	474	414	○	0.06	○	○	845	272	393	○	○
0.12	○	488	425	○	0.12	○	○	887	275	400	○	○
0.18	○	496	433	○	0.18	○	○	890	279	404	○	○
0.24	○	497	558	○	0.24	○	○	891	280	404	○	○
0.30	○	504	○	○	0.30	○	○	892	280	406	○	○

Table 1: Time when $SV_{8000} > \varepsilon_s$ for $A = 2$ and $m = 3.9$ to 4.2 , and for $A = 3$ and $m = 7.6$ to 8.2 . The left table is for $A = 2$ and the right one is for $A = 3$. ○ means that $SV_{8000} \leq \varepsilon_s$ is always satisfied for $0 \leq t \leq 1000$. The values represent the times when $SV_{8000} > \varepsilon_s$.

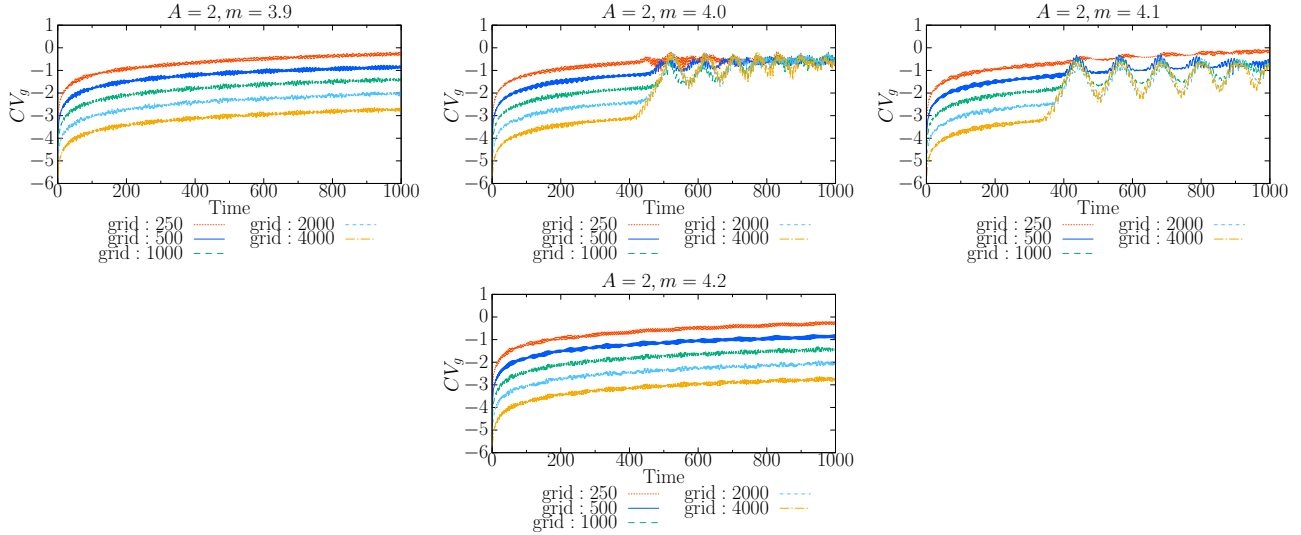


Figure 3: Relative errors between ϕ with 8000 grids and ϕ with other grid numbers when $A = 2$ and $m = 3.9$ to 4.2 . The vertical axis is CV_g and the horizontal axis is time. The top-left panel is for $m = 3.9$, the top-center one is for $m = 4.0$, the top-right one is for $m = 4.1$, and the bottom one is for $m = 4.2$. The convergence seems not satisfied at either $t \geq 400$ for $m = 4.0$ or $t \geq 350$ for $m = 4.1$.

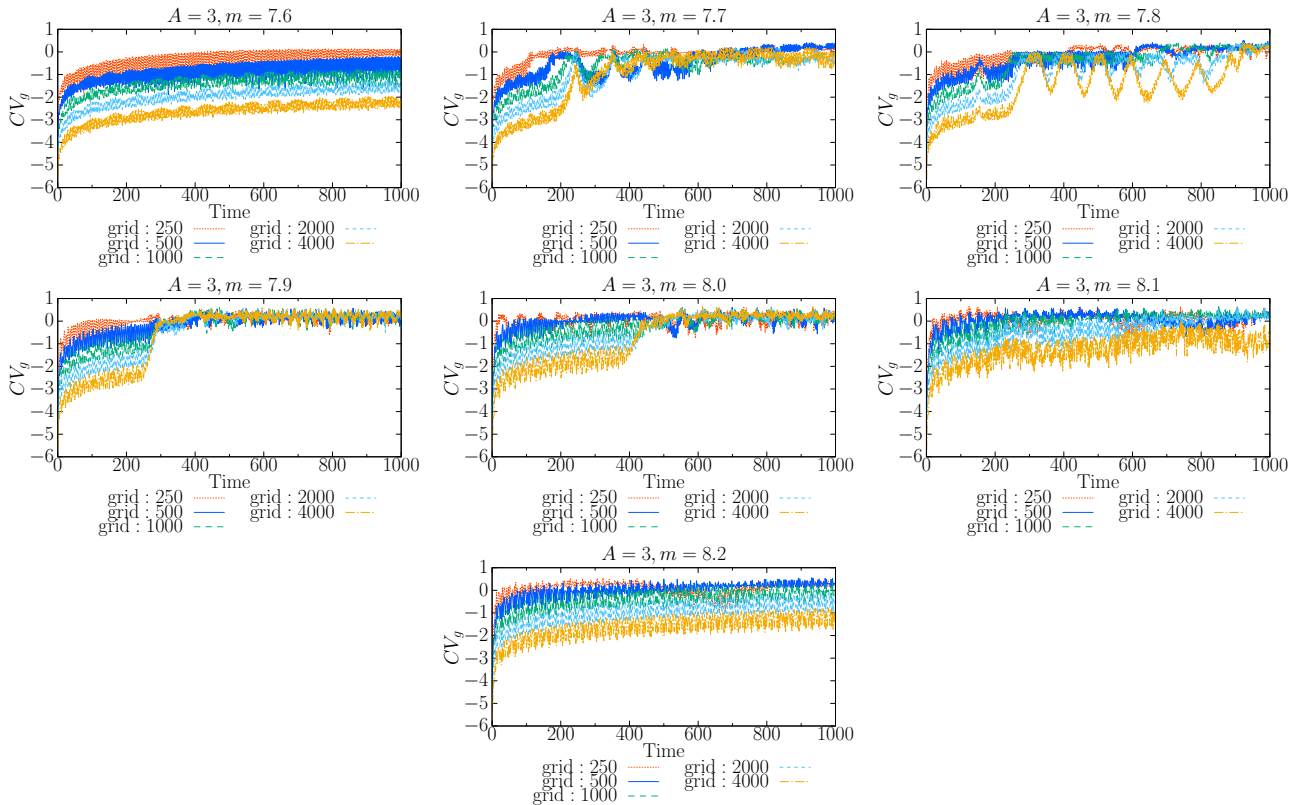


Figure 4: Relative errors between ϕ with 8000 grids and ϕ with other grid numbers when $A = 3$ and $m = 7.6$ to 8.2 . The top-left panel is for $m = 7.6$, the top-center one is for $m = 7.7$, the top-right one is for $m = 7.8$, the center-left one is for $m = 7.9$, the center one is for $m = 8.0$, the center-right one is for $m = 8.1$, and the bottom one is for $m = 8.2$. The convergence seems not satisfied at $t \geq 200$ for $m = 7.7$, at $t \geq 250$ for $m = 7.8$, at $t \geq 250$ for $m = 7.9$, at $t \geq 400$ for $m = 8.0$, or at $t \geq 250$ for $m = 8.1$.

Fig. 3 shows the convergence of ϕ for $A = 2$ and $m = 3.9$ to 4.2. The convergence seems not satisfied for either $m = 4$ or $m = 4.1$. On the other hand, Fig. 4 shows the convergence for $A = 3$ and $m = 7.6$ to 8.2. The convergence seems not satisfied for $m = 7.7$ to 8.1.

To quantitatively evaluate convergence, we calculate $DCV_g(t)$ using (12) at various ε_c values from 0.1 to 0.4. Then, $\phi_G(x) = \phi_{8000}(x)$ and $CV_G(t) = CV_{4000}(t)$ since the maximum grid number is 8000 and the second largest grid number is 4000 in these simulations. We summarize the results of the convergence in Table 2. \circ means

A = 2					A = 3							
$\varepsilon_c \backslash m$	3.9	4.0	4.1	4.2	$\varepsilon_c \backslash m$	7.6	7.7	7.8	7.9	8.0	8.1	8.2
0.1	333	423	353	450	0.1	68	41	42	28	11	17	37
0.15	\circ	431	354	\circ	0.15	942	212	149	255	107	109	276
0.2	\circ	431	354	\circ	0.2	\circ	222	239	255	241	164	530
0.25	\circ	431	363	\circ	0.25	\circ	227	244	255	330	164	745
0.3	\circ	439	363	\circ	0.3	\circ	231	251	260	396	219	\circ
0.35	\circ	439	365	\circ	0.35	\circ	270	255	261	396	219	\circ
0.4	\circ	440	365	\circ	0.4	\circ	273	256	261	396	267	\circ

Table 2: Time when $DCV_{2000} > \varepsilon_c$ for $A = 2$ and $m = 3.9$ to 4.2, and for $A = 3$ and $m = 7.6$ to 8.2. The left table is for $A = 2$ and the right one is for $A = 3$. \circ means that $DCV_{2000} \leq \varepsilon_c$ is always satisfied at $0 \leq t \leq 1000$. The values represent the times when $DCV_{2000} > \varepsilon_c$.

that $DCV_{2000} \leq \varepsilon_c$ is always satisfied at $0 \leq t \leq 1000$. On the other hand, the values represent the times when $DCV_{2000} > \varepsilon_c$.

5 Conclusion and discussion

We showed some simulations of the semilinear Klein–Gordon equation with the power-law nonlinear term in the flat spacetime. The simulations were performed using the discrete equation, which was constructed by a structure-preserving scheme for various mass m values from 3.9 to 4.2, where the amplitude of the initial value was $A = 2$ and m ranged from 7.6 to 8.2 when $A = 3$. We proposed quantitative evaluation methods for stability and convergence.

For the threshold of stability, ε_s , an appropriate value must be selected so that the time when vibration occurs in Figs. 1-2 and the time when $SV_{8000} > \varepsilon_s$ are the same, for each amplitude A . In the case of $A = 2$, from Fig. 1, the vibration appears to occur at $t \geq 500$ for $m = 4.0$ and at $t \geq 700$ for $m = 4.1$. Therefore, ε_s is adopted 0.24 for $A = 2$. In the case of $A = 3$, from Fig. 2, the vibration appears to occur at $t \geq 900$ for $m = 7.8$, at $t \geq 300$ for $m = 7.9$, and at $t \geq 400$ for $m = 8.0$. Therefore, ε_s is also adopted 0.24 for $A = 3$. On the other hand, for the threshold of convergence, ε_c , there are differences from 0.1 to 0.4 in Table 2. ε_c is a value for quantitatively judging the second-order convergence of the solutions. For $A = 2$ and 3, there is no significant change in the number of times at which $\varepsilon_c \geq 0.15$ and $\varepsilon_c \geq 0.3$, respectively. Therefore, we adopt 0.15 and 0.3 as the thresholds for $A = 2$ and 3, respectively. Regarding ε_c for $A = 3$ being greater than that for $A = 2$, this means that the convergence becomes worse as the amplitude of the initial value increases. It seems that the large initial amplitude due to the effect of nonlinear terms worsens the convergence of the solutions. Note that the appropriate values of ε_s and ε_c depend on the parameters of the numerical calculation, such as the amplitude of the initial value and the mass. Thus, we have to investigate the appropriate values of thresholds under different numerical calculation conditions.

In this study, we only investigated in the flat spacetime. What we would like to investigate next in our future work is in a curved spacetime. The range of values for m and A is limited in this paper. Future work will involve investigating the stability and convergence over a wider range of values for m and A .

Acknowledgments

T.T. and M.N. were partially supported by JSPS KAKENHI Grant Numbers 21K03354 and 24K06855. T.T. was partially supported by JSPS KAKENHI Grant Number 24K06856.

References

- [1] R. M. Wald, *General Relativity*, University of Chicago Press, Chicago, 2000.
- [2] K. Yagdjian, The semilinear Klein–Gordon equation in de Sitter spacetime, *Discrete Contin. Dyn. Syst. Ser. S*, **2** (2009), 679–696.
- [3] M. Nakamura, The Cauchy problem for semilinear Klein–Gordon equations in de Sitter spacetime, *J. Math. Anal. Appl.*, **410** (2014), 445–454.
- [4] T. Tsuchiya and M. Nakamura, On the numerical experiments of the Cauchy problem for semi-linear Klein–Gordon equations in the de Sitter spacetime, *J. Comput. Appl. Math.*, **361** (2019), 396–412.
- [5] T. Tsuchiya and M. Nakamura, Numerical simulations of semilinear Klein–Gordon equations in the de Sitter spacetime with structure preserving scheme, in: *Analysis, Applications, and Computations*, pp. 549–559, Springer International Publishing, Switzerland, 2023.
- [6] T. Tsuchiya and M. Nakamura, Numerical accuracy and stability of semilinear Klein–Gordon equation in de Sitter spacetime, *JSIAM Lett.*, **15** (2023), 45–48.